Valorization of *Sargassum Fluitans III* from the mexican caribbean: solar drying and pyrolysis

Villafán-Vidales H.I[1], López A.[1], Okoye P.U.[1], Arias Lizarraga D.[1], Arreola-Ramos C.A.[2], Chávez V.[3], Silva R.[3]

[1]*Instituto de Energías Renovables, Universidad Nacional Autónoma de México, Priv. Xochicalco S.N., Temixco, 62580, Morelos, México, Email: hivv@ier.unam.mx*

[2] *CONAHCYT, Centro de Investigación en Óptica, Prolongación Constitución 607, Aguascalientes, 20200, Aguascalientes, México.*

[3]*Instituto de Ingeniería, Universidad Nacional Autónoma de México, Ciudad Universitaria, Coyoacán, Ciudad de México, 04510, México.*

Abstract

Since 2014, the Mexican Caribbean has received more than 2360 m^3 of *Sargassum* per km of coast. This sargassum is gathered with any treatment, and in the high temperatures it decomposes rapidly, generating pollution on the seashore and health problems in the local community. This work proposes a train of solar treatment for the valorization of *Sargassum fluitans* III, which consists of drying and pyrolysis for the production of biochar. Findings show that the drying time is around 90 min, independent of the type of solar dryer (i.e., greenhouse solar dryer (GHD) or open-sun drying. Results from the pyrolysis process show that the main characteristics of the biochar are affected by the temperatures of the process. At 800 ºC, an amorphous char is obtained, with some inorganic compounds, such as potassium, sodium, phosphorus, sulfur, and chlorine, characteristics that are attractive for its use in energy storage, or as a biofertilizer.

Keywords: Concentrated solar energy, solar pyrolysis, biochar, solar drying

Resumen

Desde el 2014 el Caribe Mexico recibe mas the 2360 m3 de *Sargassum* por km de costa. Este sargassum es almacenado sin ningún tratamiento, y con las altas temperaturas se descompone rápidamente, generando contaminación en la costa y problemas de salud en la comunidad local. Este trabajo propone un tren de tratamiento solar para la valorización de *Sargassum fluitans* III, el cual consiste en el secado y la pirólisis para la producción de biocarbón. Los resultados muestran que el tiempo de secado es de aproximadamente 90 min, independientemente del tipo de secador (i.e. secador solar invernadero (GHD) o un secador solar abierto. Los resultados del proceso de pirólisis muestran que las principales características del biocarbón dependen de la temperatura del proceso. A 800 ºC, se obtiene un carbón amorfo, con algunos compuestos inorgánicos, como potasio, sodio, fósforo, azufre y cloro, caracttérisixticas que son atractivas para su uso en almacenamiento de energía o como biofertilizante.

Palabras clave: Energía Solar Concentrada, Pirólisis solar, biochar, secado solar.

1. Introduction

Since 2014, the Mexican Caribbean has received more than 2360 m^3 of Sargassum per km of coast [1]. The massive influxes are believed to be linked to human activities that have affected ocean temperatures. In 2018, the amount of Sargassum reported on the Caribbean coast was 20 million metric tons [2], which then increased, although the amount varies depending on ocean currents and on seasonal conditions. At its peak (March to August, 2018) 4500 m^3/km was being beached per month [2]. The main species are *Sargassum fluitans* III, *Sargassum natans* I and *Sargassum natans* VII, with *Sargassum fluitans* III (*S. Fluitans* III) being the dominant species, accounting for around 60% of the total biomass [3]. A range of solutions to clean up the beaches and seashore have been implemented, with mixed results. Unfortunately, sand is often removed during cleaning, and beach fauna is destroyed with severe consequences for ecological systems. Once the seaweed is collected and taken from the beach, it is usually left to accumulate in huge mounds of untreated biomass in nearby communities, where it decomposes rapidly, resulting in land and water contamination, and in health problems for the local population [4]. In order to mitigate these problems, several potential uses for the sargassum have been proposed that take advantage of it as a resource, rather than simply view it as a waste product. Examples include construction materials, such as MDF panels, adobe, and concrete [5], biofilters and adsorbents [6] and textile and pharmaceutical products [2].

All of these valorized waste products use dry biomass, which is produced via a costly, energy-intensive drying process. To reduce these costs, a solar treatment, followed by a pyrolysis process is proposed. This low-cost means of preserving the Sargassum reduces its volume and allows it to be accumulated safely, before pyrolysis is carried out, to give biochar. *S. Fluitans* III was dried in a greenhouse solar dryer (GHD), and thus, the kinetic parameters were obtained in order to design a large-scale Sargassum solar dryer. Pyrolysis was performed in two different pyrolysis reactor to valorize the Sargassum. The pyrolysis process was performed at different temperatures to evaluate the impact of temperature in the char properties.

2. Methodology

2.1 Solar drying system and process

Fresh sargassum samples were collected in Puerto Morelos, Quintana Roo, Mexico, and later classified by morphotypes, to perform a detailed evaluation of the solar pyrolysis process with different sargassum species (Figs. 1a and b). Drying tests were carried out in a greenhouse-type solar dryer (GHD) with spectrally selective films. This type of system integrates the solar and thermal drying in a closed environment with several advantages, including: reduction of product contamination, and energy consumption.

The GHD is 5 m x 6 m in area, and 4 m high, as even span greenhouse geometry. A steel structure, external and internal cover was used. The external walls are made of solid polycarbonate (PC) and consist in rear wall, front wall, and side walls. The internal walls are composed of cellular polycarbonate with spectrally selective film coating (SFC), and consist in rear internal wall, front internal wall, and side internal walls (Fig 1c). The lateral spaces between the external and internal walls prevent heat losses and to produce the airflow pattern. The spectrally selective film has two functions, the first to block UV-blue light, helping to preserve sensitive UV-light compounds, and the second to absorb the radiant energy from the sun. The drying chamber consists of three stations where the drying trays can be laid on five levels. Each station is 4 m long, and was placed 0.5 m from the front and back walls. The GHD has three inlets and three outlets for air flow (Fig.1 d). Three fans were placed 1 m from the rear wall and at a height of 2.50 m, to promote the recirculation of the air, as previously reported in Román-Roldán et al. [7]. The energy absorbed by the spectral selective film is recovered with an air flow driven by fans placed above the false ceiling. Subsequently, air is conducted into the drying chamber because the side and front walls act as deflector plates. This innovative system avoids the use of solar collectors for air heating, reducing the land area occupied and the investment cost.

The air temperature, relative humidity (RH%) and air velocity inside the dryer were continuously measured. (Fig.1 e) The air velocity was set at 1.7 ± 0.2 m/s. The environmental parameters HR_{air}%, environmental temperature (T_{amb}), global irradiance (I), and wind speed (v_w) were measured continuously using the data provided by the IER-UNAM meteorological station. Drying tests were performed at constant temperature for comparison.

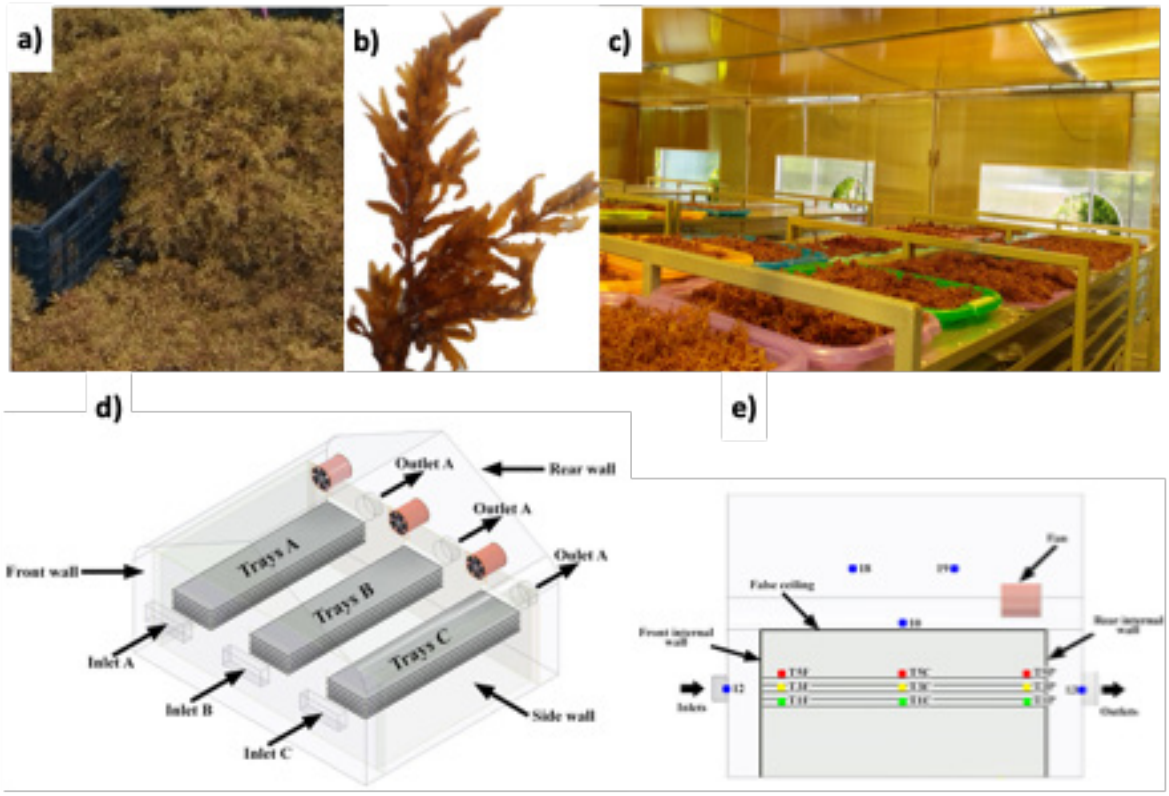

Figure 1. a) Sargassum collection stage in Puerto Morelos, Quintana Roo. b) Photograph of *S. Fluitans III*. c) New greenhouse-type solar dryer (GHD) with sargassum samples, d) Scheme of the GHD with the 3 drying stations, e) temperature, velocity and RH sensors located inside the GHD.

Two materials with specific optical properties were used as internal and external covers of the GHD. The external cover is solid polycarbonate that allow to transmit 95% of the energy of the entire solar spectrum [8]. The SFC material of the rear internal wall, front internal wall, and side internal walls allows to transmit 40% of the sun energy, from 290 nm to 1600 nm. The solar rays that fall on the internal walls and the rear internal wall absorbs 50% of the solar energy, and 10% is reflected. The solar spectral irradiance measured under the PC and with the combination of PC and SFC is shown in Figure 2.

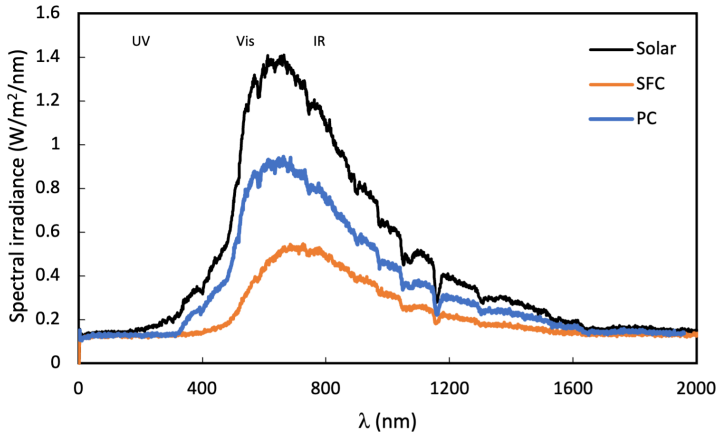

Figure 2. The spectral solar irradiance measured outside the solar dryer (solar) inside the solar dryer below the solid polycarbonate (PC), and the selective conductive film (SFC).

The weight loss of the sargassum on three drying stations of the GHD was measured every 30 minutes. In addition, open-drying tests were carried out simultaneously, for comparison. The drying kinetics was calculated using the normalized moisture content (MR) as follows:

$$MR = \frac{X - Xe}{Xo - Xe} \qquad (1)$$

Where X is the moisture content as a function of time, X_o is the moisture content at the beginning of the drying process, and X_e is the moisture content at the end of the drying .

The Arrhenius equation is used to calculate the activation energy to drive drying.

$$D_{eff} = D_o e^{\frac{E_a}{RT}} \qquad (2)$$

Where: Do is a constant (m^2/s) that describes a constant diffusivity equivalent to the diffusivity at an infinitely high temperature, Ea is the activation energy (kJ/mol), R is the general constant of the ideal gas (8.314, J / mol K), and T is the absolute drying temperature (K).

2.2 Physicochemical characterization of S. Fluitans III and biochar

Physicochemical characterization was carried out on the sample using different techniques to evaluate the chemical composition and the morphology of the raw biomass and biochar. CHNS-O elemental composition was performed on the dry S. fluitans III biomass using a Perkin Elmer PE2400 analyzer. On the other hand, a thermogravimetric analysis (TGA) of the raw biomass and biochar was carried out to analyze its decomposition in a temperature range of 50 to 900 ºC in a nitrogen atmosphere (TA, Q500). The morphology of both *S. fluitans* III and biochar was analyzed using a scanning electron microscope (S-5500 Hitachi). The biomass, biochar, and remaining ash were characterized using energy dispersive spectroscopy (EDS) coupled with a scanning electron microscope (SEM). The methodology for chemical characterization by EDS was carried out in 3 different areas of the sample, and an average of the results was obtained for each element. Finally, an X-ray diffraction (XRD) analysis of the amorphous structure of the biochar was carried out (Rigaku Ultima IV).

2.3 Solar pyrolysis

The pyrolysis process is often used to transform biomass into a variety of products. There are several ways of providing heat to the pyrolysis reactor, most of which involve the consumption of conventional fuels. This implies that a high-quality fuel is used to obtain a low quality fuel, therefore a pyrolysis process that obtains bio-oil using conventional fuels is not economically viable. Consequently, using concentrated solar energy to heat a reactor was proposed. After drying, solar pyrolysis was performed in a solar tubular reactor of 20 cm-diameter, 46 cm height. Inside the reactor there is an alumina crucible into which 2 g of *S.Fluitans* III sample was placed (Figure 2).

The pyrolysis reactor was heated using a concentrating solar system of the IER-UNAM (Solar Furnace). This furnace is composed of an heliostat of 81 m^2 that follows the sun and redirects the solar rays to the concentrator. The concentrator has 409 spherical mirrors that concentrate the solar rays at a focal distance of 3.68 m in a spot diameter of 8-9 cm. Between the solar concentrator and the heliostat, is a shutter that allows the amount of incident solar energy to be controlled and thus the temperature in the focal zone. (Fig. 3) The reactor is placed in the focal zone of the IER-UNAM Solar Furnace to reach reaction temperatures. At the beginning of the experiment, an Argon flow of 4 L/min was used for ten minutes to obtain a free-oxygen atmosphere. This flow was later reduced to 2 L/min during the experiment . The temperature was continuously monitored with a type K thermocouple. Solar pyrolysis experiments were performed at temperatures ranging from 250 °C to 800 °C for 1 hour with a heating rate of 20 °C/min to evaluate the impact of temperature in the process.

To perform a comparison of the char obtained with concentrated solar energy a pyrolysis in a tubular reactor heated by electric resistance was performed. The pyrolysis was conducted at 800 °C for 1 h at 22 °C/min heating rate. After pyrolysis, the biochar was washed with 1 M HCl to eliminate impurities, excess salts, and ashes. Subsequently, it was washed with distilled water until a pH of 7 was reached.

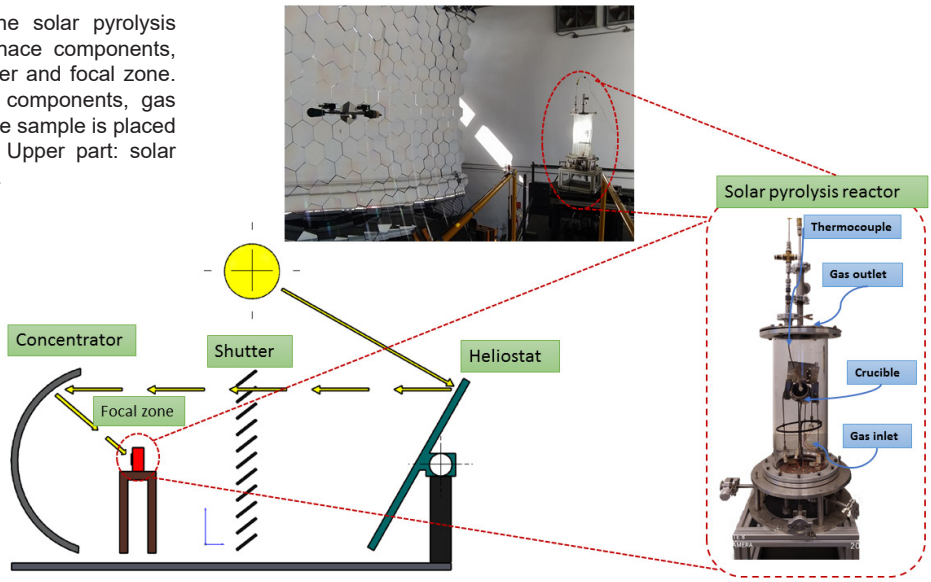

Figure 3. Schematics of the solar pyrolysis experiments. Left: Solar furnace components, Heliostat, concentrator, shutter and focal zone. Right: solar tubular reactor components, gas inlet and outlet, crucible where sample is placed and type "K" thermocouple. Upper part: solar pyrolysis reactor in operation.

3. Results

3.1. S. Fluitans III characterization

The CHNS-O elemental composition of S. Fluitans III indicates that this alga has the following composition: 26.83% carbon, 4.36% hydrogen, 1.17% nitrogen, 0.92% sulfur and 66.7% oxygen. *S. fluitans* III is 31.84% ash. The chemical EDS characterization shows the following composition: chlorine 29.76%, potassium 17.15%, calcium 10.78%, oxygen 28.09%, sodium 9.54%, sulfur 1.89% and magnesium 3.58%.

The TGA analysis (Fig. 4) shows some relevant decomposition peaks: The first mass loss (14.24 %) corresponds to water and volatiles, observed from 61 ºC to 221 ºC. The largest mass loss (34.99 %) occurs from 221 ºC to 580 ºC and corresponds to the decarbonization and degradation of polymers. The last mass loss (28.94 %) is observed from 580 ºC to 889 ºC, and it is attributed to the decomposition of organic matter and the elimination of some metals and salts [9].

3.2 Solar drying

Figure 5a shows the kinetics of the sargassum drying. The drying time is 90 minutes for all cases. There are no significant differences in the drying time of open-drying (DSD) and greenhouse drying (GHD). Nevertheless, in the middle stage of the drying, between 30 - 60 min, there are significant differences in the drying times of the two treatments. Moisture loss in trays SF1 and SF3 was faster than in tray SF2 due the reduction of air velocity at this point in the GHD. Also, the moisture loss in trays SF1 and SF3 was faster than in the DSD due the temperature and wind speed.

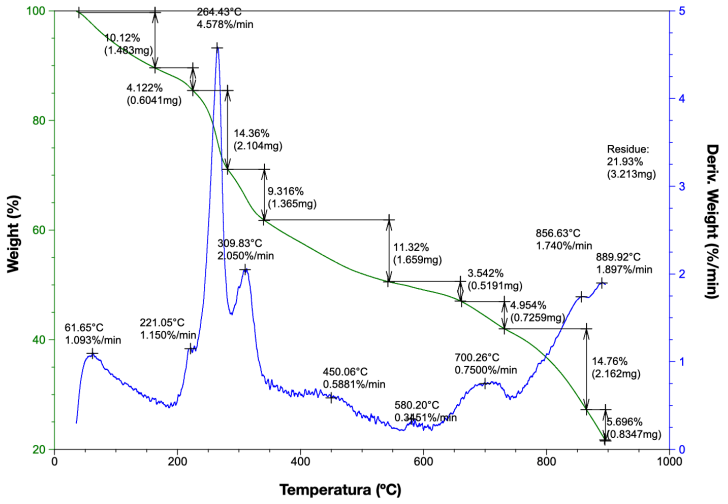

Figure 4. TGA analysis of *S. fluitans* III.

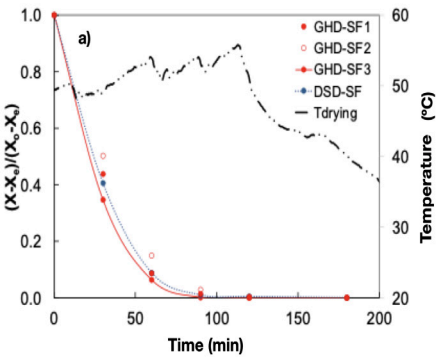

Figure 5. Drying kinetics of S. Fluitans

The average air velocity inside the GHD dryer was 1.7 m/s and the wind speed on the samples exposed directly to the sun was 2.1 m/s. The average of the relative humidity inside the solar dryer was 12.38% and outside was 32.83%. The drying of the sargassum exposed directly to the sun was favored by the speed of the wind and the concrete on which the metallic trays were placed. The effective diffusivity of the GHD was greater than that of DSD (1.82 x 10-7 m^2/s, 1.413 x 10-7 m^2/s, respectively) and both values are within the range reported for liquid diffusion. Therefore, the water migration occurs faster with GHD.

3.3 Pyrolysis

Figure 6 shows different magnifications of the micrographs of the biochar obtained at 800 °C in the electrical tubular reactor. They show a disordered surface with visible white spots, which could be attributed to the presence of inorganic elements. Magnification to 100k shows that the biochar also contains pores and slits. These channels favor biochar for a wide variety of applications, such as catalyst or adsorbent of contaminants, thanks to the favorable channels for ion transport [10]. The X-ray diffraction analysis of *S. fluitains* III biochar is shown in Figure 7a. There are two peaks, confirming that the material obtained is a carbon structure. The largest diffraction peak is around 2θ = 25º, while the second is observed at 45º, corresponding to graphite (PDF 00-041-1487). The amplitude of the two peaks confirms that the carbon obtained is amorphous. Thermogravimetric analysis (TGA) and differential thermal analysis (DTA) of *S. fluitans* III biochar are shown in Figure 7b. The first mass loss, around 50-150 °C (16.73%), can be attributed to the evaporation of moisture from the material. This mass loss shows an endothermic reaction as seen in the long? peak at this temperature. The second (3.97%) and third (2.47%) mass losses correspond to the decomposition of volatile materials. In Figure 6b the endothermic peaks corresponding to these losses can be seen.

Further mass loss above 400 °C did not produce endothermic reactions. Therefore, it can be concluded that a stable carbon material was obtained [11].

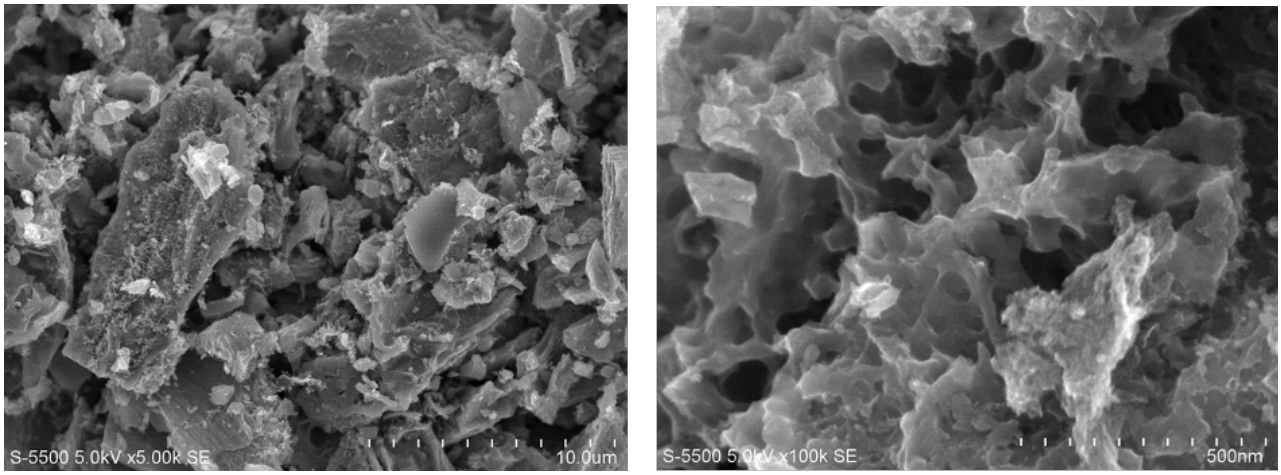

Figure 6. Micrographs of *S. fluitans* III biochar obtained at 800 °C with different magnifications.

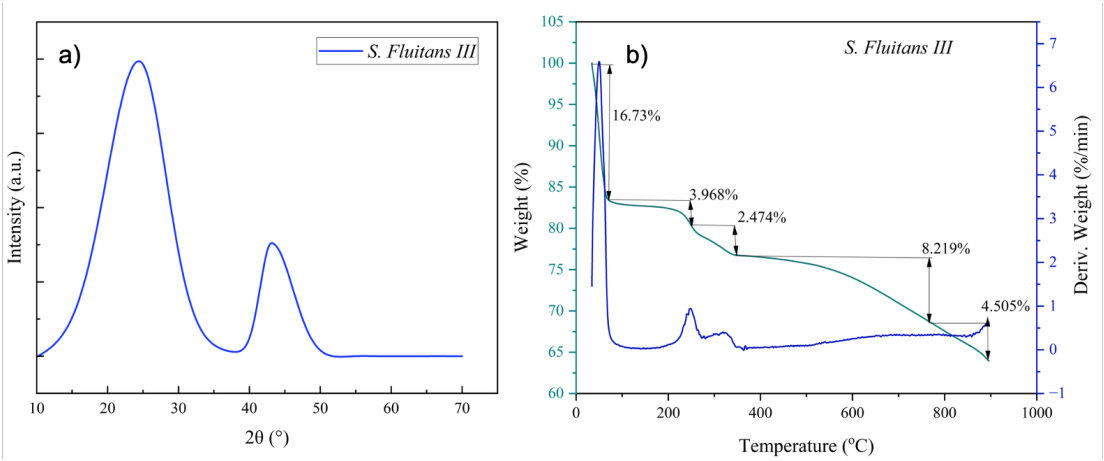

Figure 7. a) X-ray diffraction analysis of *S. fluitans* III biochar, b) TGA/DTG analysis of *S. fluitans* III biochar.

Solar pyrolysis was performed at different temperatures to assess the impact of temperature in the char yield and its main characteristics. Figure 8 shows the char yield and chemical conversion of each experiment. In this figure, it can be observed that an increase of temperature lowers the char yield from 77.2% to 29. 5%, due to the higher decomposition of *S. fluitans* III. At 800 °C, there are more cracking reactions, increasing the gas production and reducing the char yield from 50.3% to 29.5%. The metals found in the *S. fluitans* III, such as calcium and potassium, also favor tar disintegration reactions and char reforming, which increase the gas yield and reduce the char yield [12].

The results found in this work are consistent with those found in the literature. Farobie et al. [12] investigated the effect of temperature on the product distribution, where it is reported that at 400 °C, the the char yield is 55 %. When the temperature is 600 °C, the char yield falls to 30 %. In our experiments, the char yield at 400 ºC is 60%, and when the temperature increases to 650 ºC, the car yield decreases to 50%.

Two similar experiments were performed at 350 °C (Fig. 8). In this figure, minor differences, of 2% in both cases, in the char yield and chemical conversion are seen. These differences can be attributed to the minor variations in temperature that are obtained in the solar reactor, which are between 30 and 50 °C.

The micrographs of solar chars obtained at different pyrolysis temperatures are shown in Fig. 9. The raw biomass has a smooth textured wall. When the pyrolysis process is performed at 350 °C, the wall starts to break down, producing fissures. As the pyrolysis temperature increases, the structure of the raw biomass breaks more easily, resulting in a porous, amorphous structure. In the micrographs, from the EDS analysis, it is also possible to observe the inorganic compounds in the char surface (white zones of Fig. 9): chlorine, potassium, calcium, magnesium and sulfur.

The TG analysis of solar biochar is shown in Figure 10. The first mass loss at around 50-100 °C (9.47%) can be attributed to the evaporation of moisture from the material. The following mass losses (7.25 %, 5,72%, and 6.21 %) correspond to the decomposition of volatile materials. However, above 700 °C, a larger mass loss is seen (33.43 %), which may be due to a catalytic effect of alkali (K and Na) and alkaline earth metals (Ca and Mg) remaining in the char structure [13]. It can therefore be concluded further studies to evaluate the catalytic effect of metals on the physical activation of *S. fluitans* III char are required.

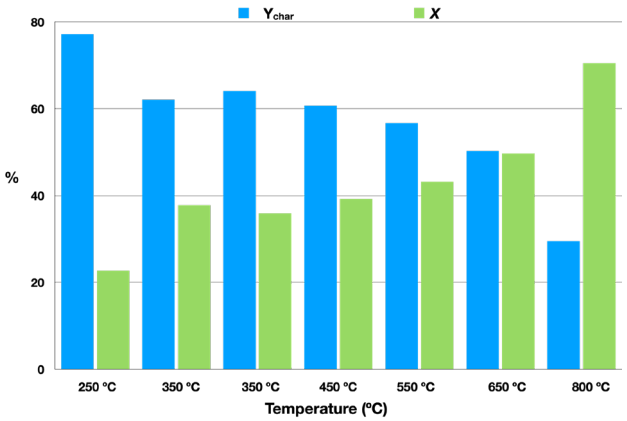

Figure 8. Solar pyrolysis experiments: temperature, char yield and chemical conversion.

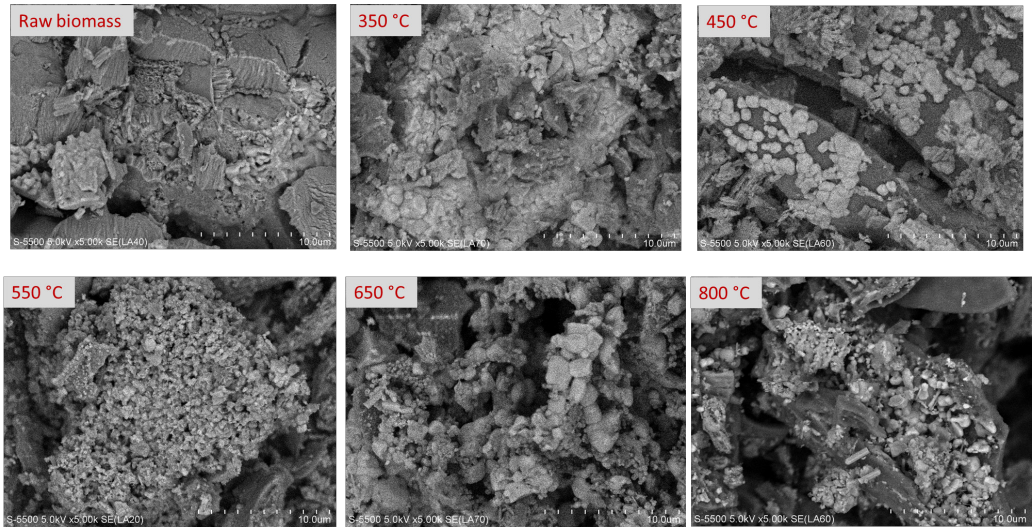

Figure 9. Micrographs of raw biomass (dry *S. fluitans* III) and solar biochar obtained at different temperatures.

The biochar obtained by both methods is amorphous and porous. Although the pores do not have a well-defined geometry, they can function as channels for ion transport or as active sites for energy storage. Inorganic components such as chlorine, potassium, calcium, sodium, magnesium and sulfur are also present. It is worth mentioning that at 800°C, a white deposit forms on the walls of the solar reactor. EDS analysis of this white deposit showed it to be composed of Cl, K, and Na, indicating that high temperatures promote the separation of some of the inorganic components of the biochar. This could be of interest for specific biochar applications. For instance, its porous, amorphous structure makes it ideal for water and air filtration systems, where the pores can adsorb contaminants. Biochar could also be used in energy storage technologies, such as supercapacitors or batteries, where its surface characteristics and ion adsorption capacity are crucial. Separating inorganic components, such as chlorine, potassium, and sodium, at high temperatures could produce purer carbons, allowing advanced materials to be manufactured, or catalysts for industrial processes.

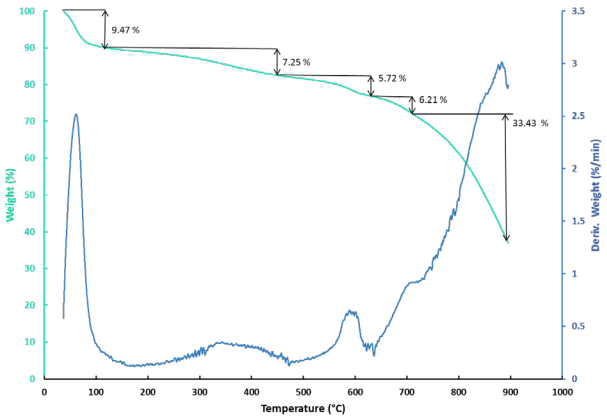

Figure 10. TGA/DTG analysis solar obtained biochar from *S. fluitans* III.

4. Conclusions

This work describes a solar treatment train for *S. fluitans* III, which consists of a two-step process: solar drying using a greenhouse-type solar dryer and pyrolysis of dried sargassum to produce biochar. This treatment train reduces the risk of sargassum decomposition and produces a value-added product, biochar, which could be used in energy storage technologies, such as supercapacitors or batteries or as biofertilizers due to the porosity and inorganic components present. The drying time was 90 minutes, whichever type of dryer is used for the conditions analyzed. In the case of pyrolysis, it was seen that increasing the temperature impacts the surface characteristics, and the carbon yield decreases, but a better quality biocarbon is obtained. The carbon obtained is amorphous, with inorganic components such as chlorine, potassium, sodium, magnesium, and sulfur. At 800 ºC, the evaporation of some inorganic components is also observed, such as Cl, K, and Na, so there is a separation process at these temperatures.

Acknowledgements

This work was funded by the project: Sostenibilidad del Caribe mexicano: Cambiando debilidades en fortalezas, of GII-IIUNAM. The authors acknowledge the technical support of Morán Elvira for the SEM and EDS analysis, Ramón-García for the XRD study, P. Altuzar for TG analysis, E. Escalante Mancera and M. Ángel Gómez Reali, for the meteorological monitoring in Puerto Morelos and to the ICML-UNAM for collecting sargassum samples.

References

[1] Vázquez-Delfín E., Freile-Pelegrín Y., Salazar-Garibay A., Serviere-Zaragoza E., Lia Méndez-Rodríguez L., Robledo D. Species composition and chemical characterization of Sargassum influx at six different locations along the Mexican Caribbean coast. Science of The Total Environment 2021, 795:148852.

https://doi.org/10.1016/j.scitotenv.2021.148852

[2] Chávez V, Uribe-Martínez A, Cuevas E, Rodríguez-Martínez RE, van Tussenbroek BI, Francisco V, Estévez M, Celis LB, Monroy-Velázquez LV, Leal-Bautista R, et al. Massive Influx of Pelagic Sargassum spp. on the Coasts of the Mexican Caribbean 2014–2020: Challenges and Opportunities. Water. 2020; 12(10):2908.

https://doi.org/10.3390/w12102908

[3] García-Sánchez M, Graham C, Vera E, Escalante-Mancera E, Álvarez-Filip L, van Tussenbroek B. Temporal changes in the composition and biomass of beached pelagic Sargassum species in the Mexican Caribbean, Aquatic Botany 2020; 167: 103275.

https://doi.org/10.1016/j.aquabot.2020.103275

[4] Resiere D., Valentino R., Nevière R., Banydeen R., Gueye P., Florentin J., Cabié A., Lebrun T., Mégarbane B., Guerrier G., Mehdaoui H. Sargassum seaweed on Caribbean islands: an international public health concern. The Lancet 2018, 392(10165)0:2691.

https://doi.org/10.1016/S0140-6736(18)32777-6

[5] Salazar-Cruz B.A., Zapien-Castillo S., Hernández-Zamora G., Rivera-Armenta J.L. Investigation of the performance of asphalt binder modified by sargassum, Construction and Building Materials 2021, 271: 121876.

https://doi.org/10.1016/j.conbuildmat.2020.121876

[6] López Miranda J.L., Celis L.B., Estévez M., Chávez V., van Tussenbroek B.I., Uribe-Martínez A., Cuevas E.,Rosillo Pantoja I., Masia L., Cauich-Kantun C., Silva R. Commercial Potential of Pelagic Sargassum spp. in Mexico. Front. Mar. Sci.,2021,8.

https://doi.org/10.3389/fmars.2021.768470

[7] Román-Roldán N.I, Ituna Yudonago J.F., López-Ortiz A, Rodríguez-Ramírez J, Sandoval-Torres S. A new air recirculation system for homogeneous solar drying: Computational fluid dynamics approach, Renewable Energy, 2021, 179: 1727-1741.

https://doi.org/10.1016/j.renene.2021.07.134

[8] López-Ortiz A., Salgado MN., Nair PK., Ortega AB., Méndez-Lagunas LL., Hernández-Díaz, WN., Guerrero L. Improved preservation of the color and bioactive compounds in strawberry pulp dried under UV-Blue blocked solar radiation. Cleaner and Circular Bioeconomy 2024: 100112.

https://doi.org/10.1016/J.CLCB.2024.100112

[9] Hussain ST, Saqib SA, Sharma TK., Nielsen AH., Pedersen TH., Rosendahl LA. Influence of Process Conditions on Hydrothermal Liquefaction of eucalyptus Biomass for Biocrude Production and Investigation of the In- organics Distribution, Sustainable Energy & Fuels 2021; 5: 1477-1487.

https://doi.org/10.1039/D0SE01634A

[10] Lobato-Peralta DR, Amaro R, Arias DM, Cuentas-Gallegos AK, Jaramillo-Quintero OA, Sebastian PJ, Okoye, PU. Activated carbon from wasp hive for aqueous electrolyte supercapacitor application. Journal of Electroanalytical Chemistry, 2021; 901:115777.

https://doi.org/10.1016/j.jelechem.2021.115777

[11] López-Sosa L., Alvarado-Flores J., Corral-Huacuz J., Aguilera-Mandujano A., Rodríguez-Martínez R., Guevara Martínez S.,Morales-Máximo M. A Prospective Study of the Exploitation of Pelagic Sargassum spp. as a Solid Biofuel Energy Source. Applied Science 2020; 10(23).

https://doi.org/10.3390/app10238706

[12] Farobie O, Amrullahc A, Bayud A, Syaftikae N, Anisb LA., Hartulistiyoso E. In-depth study of bio-oil and biochar production from macroalgae Sargassum sp. via slow pyrolysis, RSC Adv. 2022; 12: 9567-9578.

https://doi.org/10.1039/D2RA00702A

[13] Huang Y, Yin X, Wu C, Wang C, Xie J, Zhou Z, Ma L, Li H. Effects of metal catalysts on CO2 gasification reactivity of biomass char. Biotechnology Advances 2009; 27 (5): 568-572.

https://doi.org/10.1016/j.biotechadv.2009.04.013